



Optogenetic Tools for Control of Public Goods in *Saccharomyces cerevisiae*

Neydis Moreno Morales,^a Michael T. Patel,^b Cameron J. Stewart,^a Kieran Sweeney,^a  Megan N. McClean^{a,c}

^aDepartment of Biomedical Engineering, University of Wisconsin—Madison, Madison, Wisconsin, USA

^bLewis-Sigler Institute for Integrated Genomics, Princeton University, Princeton, New Jersey, USA

^cUniversity of Wisconsin Carbone Cancer Center, University of Wisconsin School of Medicine and Public Health, Madison, Wisconsin, USA

Michael T. Patel and Cameron J. Stewart contributed equally to this work.

ABSTRACT Microorganisms live in dense and diverse communities, with interactions between cells guiding community development and phenotype. The ability to perturb specific intercellular interactions in space and time provides a powerful route to determining the critical interactions and design rules for microbial communities. Approaches using optogenetic tools to modulate these interactions offer promise, as light can be exquisitely controlled in space and time. We report new plasmids for rapid integration of an optogenetic system into *Saccharomyces cerevisiae* to engineer light control of expression of a gene of interest. In a proof-of-principle study, we demonstrate the ability to control a model cooperative interaction, namely, the expression of the enzyme invertase (SUC2) which allows *S. cerevisiae* to hydrolyze sucrose and utilize it as a carbon source. We demonstrate that the strength of this cooperative interaction can be tuned in space and time by modulating light intensity and through spatial control of illumination. Spatial control of light allows cooperators and cheaters to be spatially segregated, and we show that the interplay between cooperative and inhibitory interactions in space can lead to pattern formation. Our strategy can be applied to achieve spatiotemporal control of expression of a gene of interest in *S. cerevisiae* to perturb both intercellular and interspecies interactions.

IMPORTANCE Recent advances in microbial ecology have highlighted the importance of intercellular interactions in controlling the development, composition, and resilience of microbial communities. In order to better understand the role of these interactions in governing community development, it is critical to be able to alter them in a controlled manner. Optogenetically controlled interactions offer advantages over static perturbations or chemically controlled interactions, as light can be manipulated in space and time and does not require the addition of nutrients or antibiotics. Here, we report a system for rapidly achieving light control of a gene of interest in the important model organism *Saccharomyces cerevisiae* and demonstrate that by controlling expression of the enzyme invertase, we can control cooperative interactions. This approach will be useful for understanding intercellular and interspecies interactions in natural and synthetic microbial consortia containing *S. cerevisiae* and serves as a proof of principle for implementing this approach in other consortia.

KEYWORDS optogenetics, *Saccharomyces*, public goods, invertase, microbial communities, synthetic biology

Interactions between individual cells and species dictate the development and phenotype of microbial communities (1–3). These interactions are regulated in time and space and often arise due to the different metabolic capabilities of specific cells and species (4, 5). Cooperative interactions are common, and cooperativity is often


Citation Moreno Morales N, Patel MT, Stewart CJ, Sweeney K, McClean MN. 2021.

Optogenetic tools for control of public goods in *Saccharomyces cerevisiae*. *mSphere* 6:e00581-21. <https://doi.org/10.1128/mSphere.00581-21>.

Editor Michael Lorenz, University of Texas Health Science Center

Copyright © 2021 Moreno Morales et al. This is an open-access article distributed under the terms of the [Creative Commons Attribution 4.0 International license](https://creativecommons.org/licenses/by/4.0/).

Address correspondence to Megan N. McClean, mmcclean@wisc.edu.

 Light allows temporal and spatial control of a public goods interaction in *Saccharomyces cerevisiae* @McCLeaLab

Received 24 June 2021

Accepted 1 August 2021

Published 25 August 2021

characterized by the presence of a shared public good which is produced by cooperative cells (producers) and freely available to other cells (3, 6, 7). Production of the public good is often costly, and cooperative interactions are susceptible to the presence of “cheaters,” cells which exploit the public good without providing any contribution of their own (8).

The budding yeast *Saccharomyces cerevisiae* engages in a cooperative interaction by secreting invertase, an enzyme that catalyzes the hydrolysis of sucrose into glucose and fructose. Due to its long domestication history and early enzymatic research on invertase (9–11), invertase secretion by *S. cerevisiae* has long been used as a model system for studying public good interactions and the emergence of cooperation in microbial communities. The *S. cerevisiae* genome contains several unlinked loci encoding invertase (*SUC1* to *SUC8*) (12, 13) but all except *SUC2* are located within telomere sequences (14). The strain used in this study (S288C) carries a gene that encodes only one functional invertase enzyme, *SUC2* (12, 15). There is a constitutively expressed intracellular form of invertase, but the secreted, glycosylated form which is regulated by glucose repression and important for cooperativity is secreted into the periplasmic space (16). Most invertase (95%) remains in the cell wall; nevertheless, yeast capture only a small fraction of the sugars that sucrose hydrolysis releases with most of the glucose and fructose diffusing away to be utilized by other cells (17–19). Hence, the sugars produced from sucrose hydrolysis represent a “public good.” Invertase is costly to produce, and producing populations are susceptible to invasion by cheaters (17, 20).

There is growing evidence from both experiments and simulations that when and where a public good is produced within a microbial community can have dramatic consequences for community stability and the maintenance of cooperativity (21–27). The spatial arrangement of genotypes within microbial communities can influence whether or not producers sufficiently benefit from the production of public goods or whether cheaters are able to invade and take over the community (3, 26, 28–30). Indeed, efficient use of public goods has been identified as a possible driver for the evolution of multicellularity (31). Furthermore, the dynamic control of public goods in both space and time could be used to manipulate synthetic consortia for applications in bioproduction and biotechnology (32, 33). Yet, few tools exist for spatiotemporal control of specific community interactions.

Optogenetic tools offer the potential to overcome this limitation by utilizing genetically encoded light-sensitive proteins to actuate processes within the cell in a light-dependent manner. Light is a powerful actuator, as it is inexpensive, easily controlled in time and space, and *S. cerevisiae* contains no known native photoreceptors (34). Light can be rapidly added and removed from cell cultures or spatially targeted (35–38), meaning it can be used to study how regulation of microbial interactions determines microbial community development (39–41). We report here the development of an optogenetic tool that allows the expression of a specific metabolic enzyme of interest to be put under light control in *S. cerevisiae*. Using this system, we demonstrate that we can use light to control when and where invertase is expressed within well-mixed and spatially organized populations of *S. cerevisiae*. Light control of this cooperative interaction shows that invertase expression in a community of yeast has important effects on overall community growth and spatial structure. Our results suggest that optogenetic control of microbial interactions is an important new approach to understanding and engineering microbial communities.

RESULTS

Plasmid design and system overview. To enable light-based control of cooperativity, we first developed constructs that, when integrated into yeast, allow us to make expression of a specific gene light inducible. We generated an integrable cassette containing the essential components of a blue light reconstituted transcription factor. We chose to use a split transcription factor consisting of a DNA-binding domain (DBD) fused to the naturally occurring *Arabidopsis* cryptochrome CRY2 photolyase domain (DBD-CRY2PHR)

and the CIB1 protein fused to the VP16 activation domain (VP16-CIB1). In response to blue light, CRY2 undergoes a conformational change that allows it to bind CIB1, which recruits the VP16 activation domain to a promoter of interest containing binding sites for the selected DNA-binding domain driving gene expression. We chose the DNA-binding domain of the Zif268 transcription factor (ZDBD), which is known to bind a 9-bp site (GCGTGGGCG) that has only 11 predicted binding sites in the *S. cerevisiae* genome (42). Studies using the ZDBD on an estradiol-inducible transcription factor have shown that artificial transcriptional activators using this DNA-binding domain in *S. cerevisiae* generate very little off-target gene expression activity (42, 43). When the Zif268 DNA-binding domain is fused to CRY2PHR, the resulting ZDBD-CRY2PHR/VP16-CIB1 transcription factor controls the expression of yeast genes under a pZF(BS) promoter containing GCGTGGGCG binding sites (BS) in a blue light-dependent manner (43).

Stable integration of the ZDBD-CRY2PHR/VP16-CIB1 transcription factor is a more promising approach than maintenance of the optogenetic components on episomal plasmids, as expression from plasmids is known to be noisy and requires constant selection (44). In order to integrate the ZDBD-CRY2PHR/VP16-CIB1 optogenetic machinery without loss of a marker, we used the heterologous URA3 from *Kluyveromyces lactis* (KIURA3) flanked by two direct repeats of the loxP sequence to allow for Cre recombinase-mediated marker excision (45). The components were cloned as indicated in Fig. 1A using standard cloning techniques as described in Materials and Methods. Homology arms on either side of the cassette allow for rapid integration at the *HO* locus, which is not required for growth and does not have an effect on growth rate (46, 47). We also included spacer DNA of approximately the same length (1.4 kb) as KIURA3 (1.5 kb) as indicated in Fig. 1A based on initial tests of the scheme which indicated that the spacing between the two open reading frames encoding the split transcription factor is important for optimal function of the optogenetic system (see Fig. S1 in the supplemental material).

Integration of the ZDBD-CRY2PHR/VP16-CIB1 machinery at *HO* enables light-dependent expression from the pZF(3BS) promoter in cultures grown in liquid media and on solid media (Fig. 1B and Fig. S2). Excision of the KIURA3 marker still results in some attenuation of gene expression in the marker recycled strain (Fig. 1B). We hypothesize that this is due to repression of ZDBD-CRY2PHR expression by the strongly expressed upstream VP16-CIB1 gene (Fig. 1A). This could be due to terminator-promoter interactions as previously reported (48, 49). Previous work has shown that the ratio of CRY2PHR to CIB1 in the split transcription factor is important for maximal gene expression (43), and it is possible that removing the KIURA3 marker changes the ratio to be slightly less favorable. We note that using higher light intensities (Fig. S3A) increases gene expression and that significant expression does not require a multicopy reporter plasmid (Fig. S3B). In subsequent experiments, the reduced expression due to excision of the KIURA3 marker did not cause difficulties, but we note that if maximal gene expression is required, constructs designed to optimize the dosage of VP16-CIB1 and ZDBD-CRY2PHR have been described (43).

To allow specific genes in the yeast genome to be optogenetically controlled, we designed a cassette containing a pZF(BS) promoter (5'→3') and the KanMX cassette (3'→5') (Fig. S4A), which confers resistance to the G418 antibiotic (50). Replacing an endogenous promoter with this cassette in a strain containing the ZDBD-CRY2PHR/VP16-CIB1 split transcription factor puts expression of the gene of interest under blue light control. We verified that in the dark, replacement of the native promoter with pZF(BS) effectively generates a deletion. Replacement of the *HIS3* promoter with this cassette generates a histidine auxotroph (*his3*⁻) in the dark, and the ability to grow without histidine is recovered when grown in blue light in the presence of the ZDBD-CRY2PHR/VP16-CIB1 split transcription factor (Fig. S5A). Gene expression from this promoter is rapid (sevenfold gene expression in 2 h) as assessed by pZF(BS)-yEVENUS (Fig. S4B). In combination, the cassettes containing an integrable light-responsive split

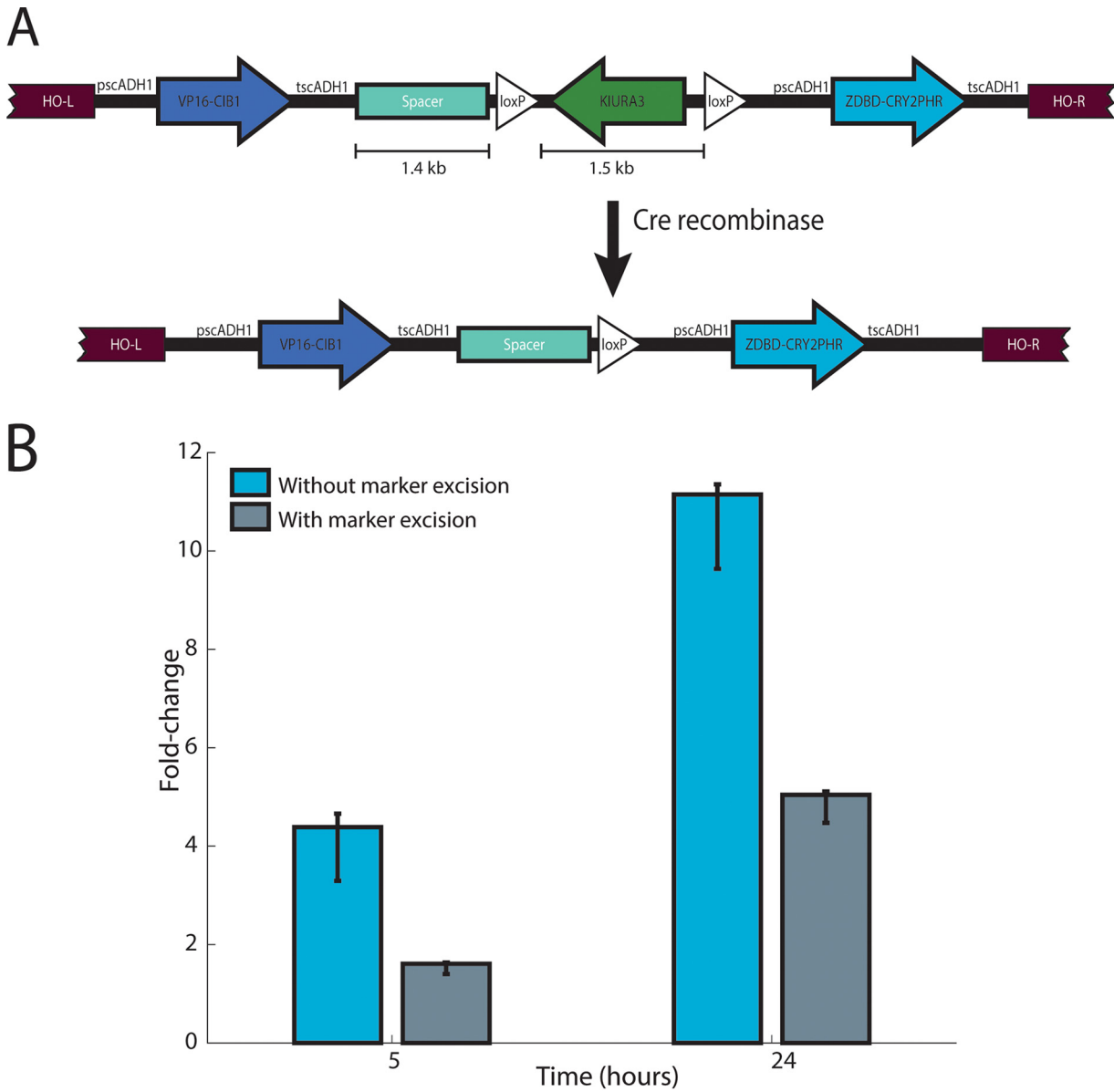


FIG 1 Characterization of vectors to integrate the blue-light-inducible split transcription factor (ZDBD-CRY2PHR/CIB1-VP16) into yeast with marker recovery. (A) The split transcription factor (TF) vector inserts ZDBD-CRY2PHR and VP16-CIB1 at the *HO* locus under the expression of constitutive (pADH1) promoters with KIURA3 selection. Expression of Cre recombinase and recombination of the loxP sites remove the KIURA3 marker, leaving it available for future strain manipulation. (B) Illumination of strains with ZDBD-CRY2PHR/CIB1-VP16 and a pZF(3BS)-yEVENUS reporter at 460 nm ($50 \mu\text{W}/\text{cm}^2$) demonstrates that the ZDBD-CRY2PHR/CIB1-VP16 transcription factor drives gene expression from the pZF promoter in strains with or without recycling of the KIURA3 marker. However, removal of the KIURA3 marker does reduce expression from the pZF promoter approximately twofold. Expression of yEVENUS was measured using imaging cytometry. Error bars depict bootstrapped 95% confidence intervals for the mean expression level.

transcription factor (ZDBD-CRY2PHR/VP16-CIB1) and a drug-selectable promoter cassette [KanMX4-pZF(3BS)] allow expression of a gene of interest to be put under light control in a variety of *S. cerevisiae* strains.

Creation of a light-inducible invertase *S. cerevisiae* strain. We decided to take advantage of the well-understood invertase public good system in budding yeast to generate yeast strains where cooperative intercellular interactions could be controlled by light (Fig. 2A). In a yeast strain with the ZDBD-CRY2PHR/VP16-CIB1 optogenetic system stably integrated at *HO*, we replaced the *SUC2* promoter with pZF(3BS) [using the KanMX-pZF(3BS) cassette]. Lawns of strains plated on yeast peptone medium with sucrose (YP-sucrose) (see Materials and Methods) were able to grow in blue light, but not

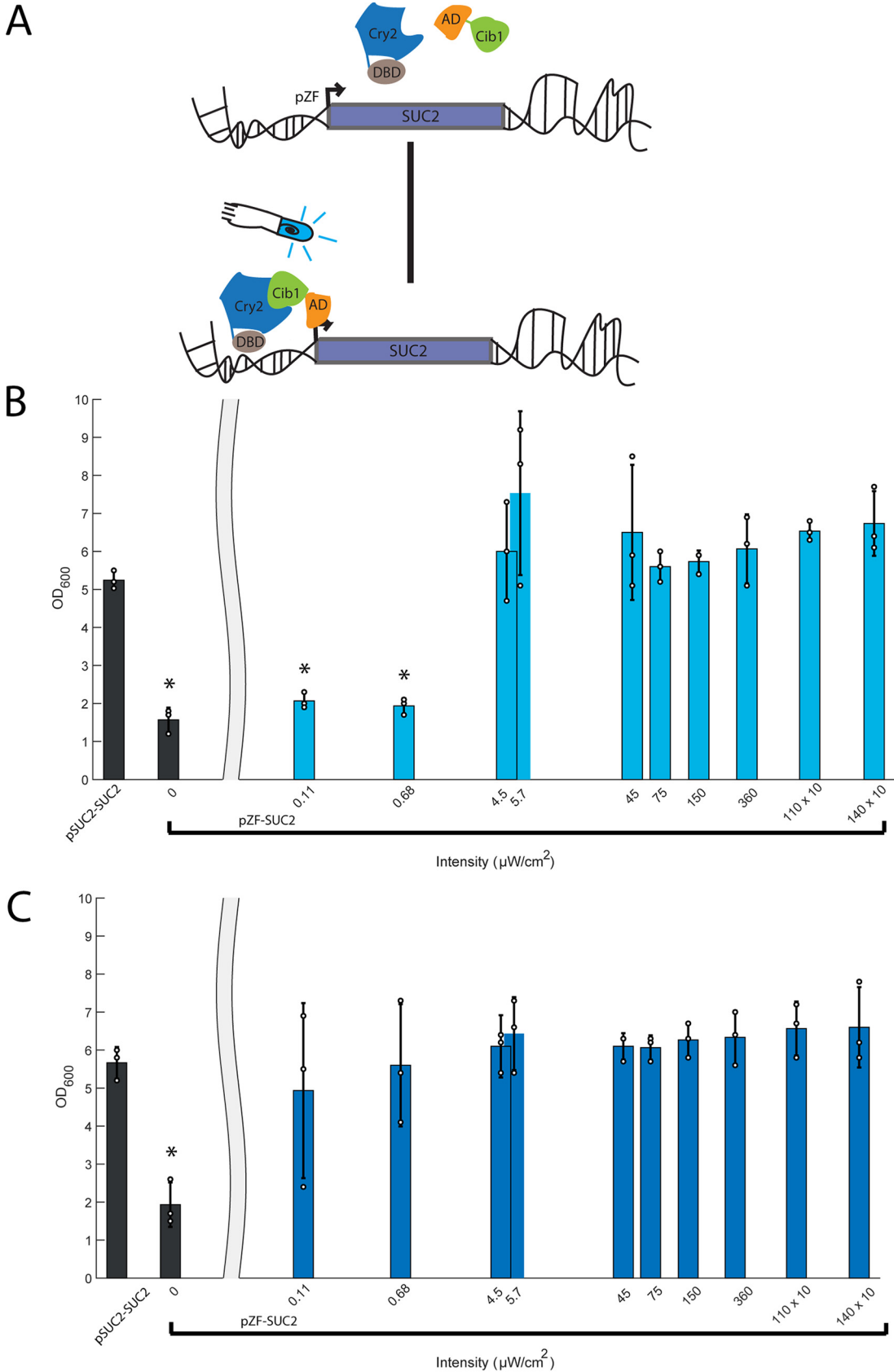


FIG 2 Characterization of a light-inducible invertase strain. (A) In a yeast strain containing the ZBD-CRY2PHR/VP16-CIB1 gene cassette, the invertase endogenous promoter (pSUC2) was substituted with the orthogonal light-inducible promoter (Continued on next page)

in the dark (Fig. S5B) indicating that these strains induced SUC2 in a light-dependent manner, allowing the cells to produce invertase and utilize sucrose.

We further tested the ability of this strain to recover growth on YP-sucrose in liquid cultures exposed to blue light. We grew cultures over a range of light intensities ($0 \mu\text{W}/\text{cm}^2$ to $14 \times 10^2 \mu\text{W}/\text{cm}^2$) and measured optical density after 24 and 48 h of growth (Fig. 2B and C). The parent strain (SUC2) quickly saturated at both 24 and 48 h. In contrast, the pZF-SUC2 strain showed very little growth after both 24 and 48 h of growth in the dark. Increasing intensity of blue light led to saturating optical densities at both 24 and 48 h. Interestingly, at high light intensities ($>4 \mu\text{W}/\text{cm}^2$), we reproducibly observed that pZF-SUC2 cultures reached a higher density than the wild-type pSUC2-SUC2 parent strain (yMM1146). It is possible that by decoupling production of invertase from the native regulation, the light-inducible strains overproduced invertase and are hence able to access more carbon from the sucrose. At low intensities of light (Fig. 2B, $0.110 \mu\text{W}/\text{cm}^2$ and $0.680 \mu\text{W}/\text{cm}^2$), the culture did not show significant growth at 24 h but by 48 h was able to reach a wild-type level of saturation. This could be due to the known Allee effect (51–54) (density-dependent growth) caused by the cooperative metabolism of sucrose by secreted invertase. At low intensities of light, low invertase production and secretion slow sucrose hydrolysis and population growth, delaying the point (relative to higher light intensity cultures) at which the population reaches a density that supports the maximal growth rate.

We further tested the induction dynamics of our light-inducible strain over a several day growth experiment (Fig. 3). The wild-type SUC2 strain quickly saturated after 20 h of growth, while the pZF-SUC2 strain had a delayed lag period, relative to the wild-type strain, which we interpret in light of the data in Fig. 2B as time needed to accumulate invertase and glucose in the medium after light induction. Subsequent to initiation of growth, the pZF-SUC2 strain showed very similar growth kinetics to the wild-type strain and quickly reached saturation. Again, the pZF-SUC2 reached a higher density than the wild-type strain at saturation, as we previously observed (Fig. 3). Interestingly, the pZF-SUC2 strain also showed some growth in the dark, albeit after an extremely delayed lag period. We know from previous studies (43) that the pZF promoter is not absolutely silent, and therefore, we interpret this growth as being due to an extremely slow accumulation of functional invertase and hexose due to leakiness from the pZF promoter. We confirmed that our sampling method did not inadvertently expose cultures to unwanted light by demonstrating that the final densities of our time course samples did not show any significant difference relative to untouched endpoint samples (Fig. S6).

Light patterning allows for spatial control of producer populations. The experiments described above demonstrate that we can control invertase production, and therefore cooperativity, with blue light. However, these experiments were all done in well mixed populations, while microbial communities are generally highly structured two-dimensional or three-dimensional environments. Therefore, we wanted to test our ability to spatially control cooperativity in populations of *S. cerevisiae*.

Localized illumination of a regular grid of pZF-SUC2 strains arrayed onto an agar pad demonstrated that a small, spatially localized group of cooperators (Fig. S7A) can support growth of a much larger number of cheaters in two-dimensional environments. This is expected due to diffusion of hexose. While the invertase enzyme is anchored to the plasma membrane, the fructose and glucose converted by the enzyme is free to diffuse, and a relatively small fraction is captured by the cell that makes it (17). To further validate this technique, we generated plates containing a lawn of pZF-SUC2

FIG 2 Legend (Continued)

(pZF) using the KanMX-pZF(3BS) cassette. In the dark, chimeric proteins ZDBD-CRY2PHR and VP16-CIB1 remain unbound and are inactive. Upon the addition of light, CRY2 undergoes a conformational change that allows binding to CIB1 and recruits VP16-CIB1 to the promoter to drive transcription. The optogenetic strain pZF-SUC2 was exposed to a range of light intensities ($0 \mu\text{W}/\text{cm}^2$ to $14 \times 10^2 \mu\text{W}/\text{cm}^2$) in YP-sucrose media. (B) At 24 h, the wild-type strain (pSUC2-SUC2) shows robust growth, while the control (pZF-SUC2, $0 \mu\text{W}/\text{cm}^2$) does not. When provided a sufficient light dose, the pZF-SUC2 strain is able to recover wild-type growth in 24 h (intensities of $>4 \mu\text{W}/\text{cm}^2$) (C) After 48 h, all pZF-SUC2 strains exposed to light catch up to the wild-type (pSUC2-SUC2) strain. Each bar represents three biological replicates, and the individual data points are shown. (*, $P < 0.05$, two-way analysis of variance [ANOVA]).

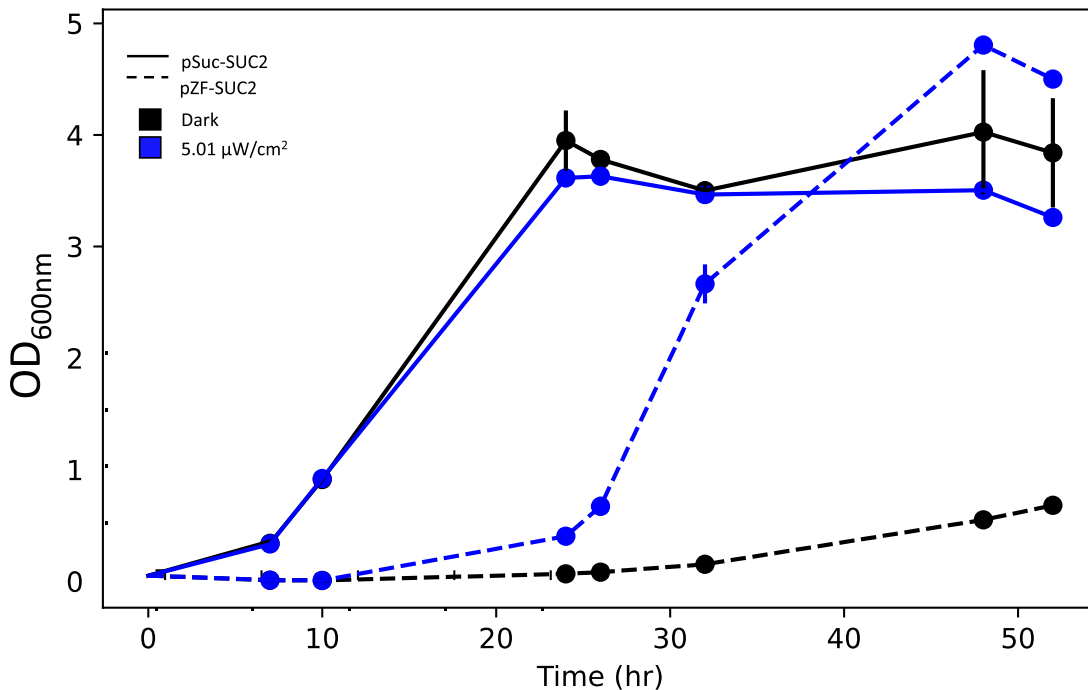


FIG 3 Light induction time course of light-inducible strain (pZF-SUC2, dashed line) and wild-type strain (pSUC2-SUC2, solid line). Light intensities are $5.01 \mu\text{W}/\text{cm}^2$ (blue) and $0 \mu\text{W}/\text{cm}^2$ light (black) ($n=2$). Error bars depict standard deviations. Error bars that are not visible are smaller than the marker. The optogenetically controlled strain displays a long lag in growth, which may be due to the time needed to accumulate invertase and break down sucrose to support growth after light induction.

cells and illuminated a spot through a 6-mm pinhole (Fig. 4A). We found that after 4 days, the growth of very few cheaters was supported, with the majority of growth visible within the illuminated region. However, after 7 days of illumination, the cooperating cells supported a large growth of cheaters presumably because they were continuing to produce invertase and hydrolyze sucrose to hexose and the majority of hexose diffuses away from the illuminated cells (i.e., the producers).

Spatial patterning due to spatial segregation of cooperators and nutrient competition. In our pinhole experiment, we noticed a subtle ring effect (Fig. 4B, Day 7), where the illuminated cooperators (at the center) grew well, surrounded by a ring of lesser growth, and finally more dense growth of cheaters at the periphery of the entire colony. This kind of ring-like pattern formation is predicted in reaction-diffusion systems where an activator and an inhibitor diffuse from a central source on different

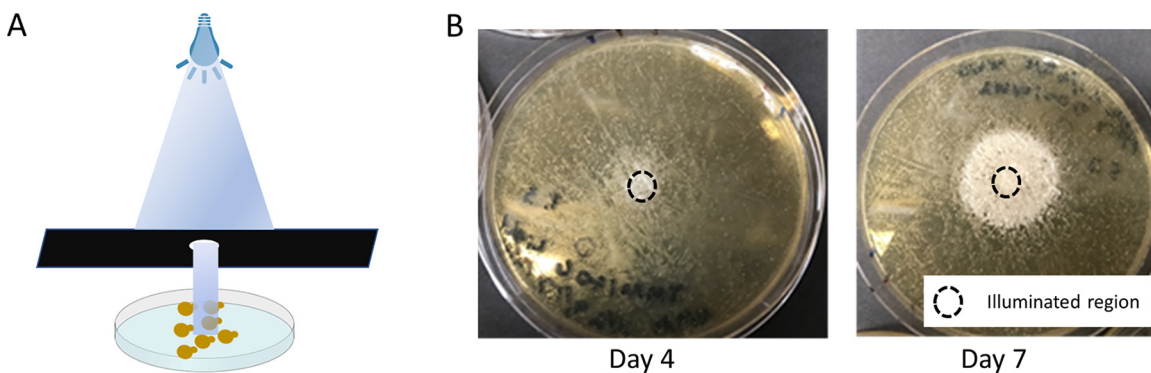


FIG 4 Controlled light results in patterned growth of a synthetic public good community. (A) Spatial patterning of our public good communities can be achieved by optogenetically controlling invertase expression in an illuminated area. A photomask limits the illuminated area on a petri plate, resulting in patterned growth. (B) A representative image of the public good community patterned on a standard petri plate. The black circle denotes the illuminated area of the plate. Growth was imaged on day 4 and day 7.

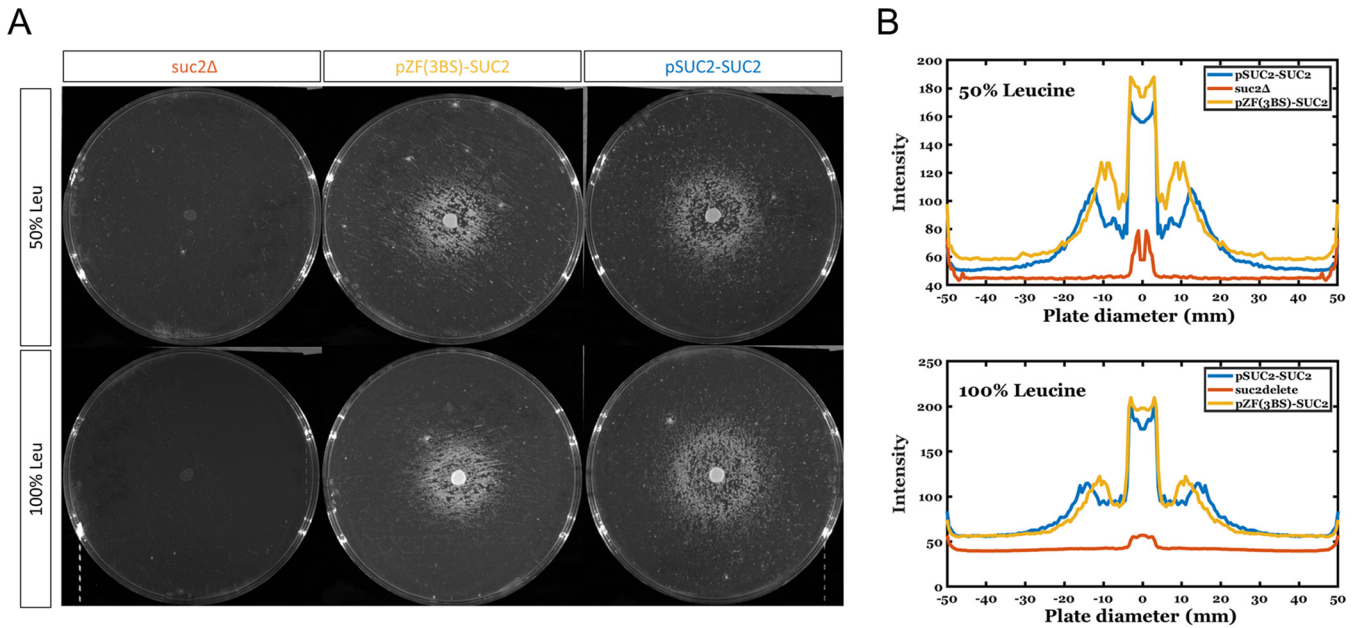


FIG 5 Spot patterning assay on nutrient-limited SC-sucrose plates. (A) Representative images of spot assay plates. The top row is composed of 50% leucine plates, while the bottom row shows the 100% leucine condition. All plates were spread with the constitutive cheater strain, *suc2Δ leu2Δ* strain. From left to right, the spotted strains are *suc2Δ leu2Δ*, pZF-SUC2, and pSUC2-SUC2. (B) Plots showing an averaged radial intensity profile of the spotted plates across the diameter of the plate. At both concentrations of leucine, the pSUC2-SUC2 strain (blue) shows a larger inhibition of growth zone than the pZF-SUC2 (yellow) strain. In all cases, there is no growth of the *suc2Δ leu2Δ* (orange) strain.

time scales (55–58). In our system, the central cooperators are activating the growth of cheaters by producing hexose while simultaneously inhibiting the growth of cheaters by serving as a sink for other limiting growth factors (i.e., nutrients) (55–57). Cheaters growing near the initially faster growing cooperators have access to hexose but are deprived of other nutrients, while cheaters at the periphery have more access to the limiting nutrient in the plate and eventually have access to hexose diffusing from the central cooperators, and therefore grow to a higher density.

In order to more fully explore this observation, we used auxotrophic strains to allow control of a limiting nutrient on the plates. Our wild-type pSUC2-SUC2 and opto-control pZF-SUC2 strains are *leu2* auxotrophs, allowing us to control leucine amino acid concentration in the plates to limit a nutrient. For a control, we generated a constitutive *suc2Δ leu2Δ* cheater strain. We spotted *suc2Δ leu2Δ* cheaters, pZF-SUC2, or pSUC2-SUC2 cells onto lawns of *suc2Δ leu2Δ* cheaters. Leucine concentrations in the plates were chosen to be 100% (0.1 mg/ml) or 50% (0.05 mg/ml) of the amount used in standard synthetic media (59). As expected, spotting *suc2Δ leu2Δ* cheaters onto a lawn of *suc2Δ leu2Δ* cheaters does not allow for any growth in either light or dark (Fig. 5A). In contrast, both pZF-SUC2 or wild-type pSUC2-SUC2 cells spotted onto cheaters and grown in blue light allows for clear growth of the cooperators (either pZF-SUC2 or wild-type) surrounded by a zone where growth of the *suc2Δ leu2Δ* cheaters is inhibited and a larger ring of dense cheater growth (Fig. 5A and B). The growth inhibition zone is larger for wild-type cooperators than pZF-SUC2 cooperators (Fig. 5B and Fig. S7B and S8). We interpret this to be due to more rapid induction of invertase and glucose production in the wild-type strains, which allows the wild-type strain to more quickly reach a high density of cooperators, allowing further cooperator growth (as also seen in Fig. 3) and greater utilization and depletion of leucine. That leucine is the limiting nutrient is evidenced by lesser growth in both the wild-type and pZF-SUC2 strains at 50% leucine than at 100% leucine (Fig. S7B and S8).

DISCUSSION

This study develops and demonstrates the use of an optogenetic tool to control cooperation in a yeast microbial community. By making expression of invertase

(encoded by the *SUC2* gene) light controllable, we demonstrate temporal and spatial control of public good production. We show that the timing of invertase expression is important, and delays in expression can significantly slow community growth. In addition, we show that localized cooperation can generate distinct patterning of cooperators and cheaters. Despite frequent investigation of *Saccharomyces cerevisiae* invertase secretion as a model cooperative community, most models approximate invertase production as constant in time and space despite known native regulation in response to external factors such as nutrient concentration (60, 61). Optogenetic control of invertase will allow for further dissection of how regulation of this enzyme in space and time allows cooperators to coexist and compete with cheaters. While we have focused on the control of an intercellular interaction, the optogenetic constructs and strains generated in this study can be immediately used by other researchers to put any gene of interest under the control of blue light in *S. cerevisiae*. The optogenetic system is orthogonal to native regulatory systems (43) and could be easily modified to utilize additional markers or CRISPR technology for integration into a variety of yeast strains or species.

More generally, this study suggests that optogenetics will be a powerful tool for understanding how spatiotemporal regulation of cooperation, and other interactions, control microbial community structure and phenotype. Interactions in microbial communities are mediated by diffusible compounds, and numerous studies indicate that short-range interactions on the micron-to-millimeter scale are important for controlling community structure and phenotype (62–64). However, controlling the spatial arrangement of microbes on these length scales can be challenging. Microfluidic devices allow spatial segregation of microbes at different length scales but require sophisticated engineering and specialized equipment (65–68). In addition, it is more challenging to define three-dimensional structure using a microfluidic device, and collection of the community for subsequent downstream analysis (e.g., gene expression) can be difficult. Bioprinting is a burgeoning technique which holds promise for building complex, three-dimensional microbial communities with defined spatial structure (65, 69–71). However, bioprinting does not easily allow intercellular and interspecies interactions to be modulated in time. Optogenetics has the potential to be integrated with or to supersede these existing technologies for fine spatiotemporal control of community interactions. Scanning and parallel light-targeting methods can be combined with one and multiphoton excitation to precisely localize light in both two and three dimensions as well as in time. In addition, existing illumination techniques can be combined with amenable animal models, such as *Caenorhabditis elegans* (72), to allow unprecedented *in vivo* dissection of the importance of intercellular interactions and their regulation in the establishment and phenotype of microbial communities. To extend the techniques described in this article to mixed-kingdom communities, optogenetic systems developed for bacteria (73, 74) could be utilized. Indeed, in *Sinorhizobium meliloti*, a nitrogen-fixing soil bacterium, the blue light-sensitive transcription factor EL222 was recently used to control production of the public good exopolysaccharide, enabling manipulation of biofilm formation (41). Hybrid optochemical approaches also hold promise for repurposing existing inducible systems, as a recent study showed that photocaged isopropyl- β -D-thiogalactopyranoside (IPTG) could be used to control co-culture interactions in the bacterium *Corynebacterium glutamicum* (39).

Finally, in addition to providing a path toward understanding how intercellular interactions regulate naturally occurring microbial communities, optogenetic tools have important implications for engineering synthetic microbial consortia. Engineered consortia are of great interest in biotechnology because they can perform more complicated functions than single-species or single-strain communities (75). However, maintaining the appropriate ratio of different consortium members represents a challenge and would benefit from dynamic control modalities. Control mechanisms for cocultures via interspecies interactions (such as quorum sensing and metabolite exchange) have been described (76–78), and dynamic control of these interactions using optogenetics and predictive control strategies (36, 79) could enable community maintenance and optimization. Similar

optogenetic approaches in monocultures have already enabled significant gains in bio-production (35, 80, 81). In addition, the spatial control provided by light could allow the formation of sophisticated living biomaterials. Cocultures of *Saccharomyces cerevisiae* and the cellulose-producing *Komagataeibacter rhaeticus* bacteria are mediated by yeast invertase production and capable of producing functionalized cellulose biomaterials. Optogenetic control of *S. cerevisiae* invertase production could allow for sophisticated control of these living materials as well as patterning, as demonstrated in this work for the simple case of localized producers. In addition, as demonstrated by the grid experiment (see Fig. S7A in the supplemental material), a small number of producers can support a much larger population, indicating that in living materials, it may be possible to have a relatively small population responsible for the metabolic burden of consortia growth, while other members can focus on additional functionality.

MATERIALS AND METHODS

Yeast strains and culture methods. Yeast strains used in this study are shown in Table S1 in the supplemental material. Yeast transformation was accomplished using standard lithium acetate transformation (82). For integrating plasmids, the integration was validated using either colony PCR or when colony PCR proved difficult, by PCR of genomic DNA. Genomic DNA was extracted using the Bst n' Grab protocol (83). Primers used for validating integrations are listed in Table S1. All transformants were checked for the petite phenotype by growth on YEP-glycerol (1% [wt/vol] Bacto yeast extract [catalog no. 212750; BD Biosciences], 2% [wt/vol] Bacto peptone [catalog no. 211677; BD Biosciences], 3% [vol/vol] glycerol [catalog no. BP229-1; Fisher Bioreagents], 2% [wt/vol] Bacto agar [catalog no. 214030; BD Biosciences] (22). Only strains deemed respiration competent by growth on YEP-glycerol were used for subsequent analysis. Details of individual strain construction are described in Text S1 in the supplemental material.

Yeast cultures were grown in either yeast peptone (YP) medium (10 g/liter Bacto yeast extract, 20 g/liter Bacto peptone for solid medium plus 20 g/liter of Bacto agar) or synthetic complete (SC) medium (6.7 g/liter yeast nitrogen base without amino acids [DOT Scientific], 1% [vol/vol] KS amino acid supplement without appropriate amino acids). The carbon source supplied was either dextrose (D) or sucrose (SUC) at 2% (vol/vol) concentration. As needed, episomal plasmids were maintained by growing yeast in SC medium lacking the appropriate amino acids required for plasmid selection. For light induction experiments followed by fluorescence assays (flow cytometry or microscopy), yeast was always grown in synthetic complete medium (59).

Bacterial strains and growth media. *Escherichia coli* strain DH5 α was used for all transformation and plasmid maintenance in this study. *E. coli* was made chemically competent following either the Inoue method (84) or using the Zymo Research Mix & Go! Protocol (catalog no. T3002; Zymo Research). *E. coli* was grown on LB agar (10% [wt/vol] Bacto tryptone, 5% [wt/vol] Bacto yeast extract, 5% [wt/vol] NaCl, 15% [wt/vol] Bacto agar) or LB liquid medium (10% [wt/vol] Bacto tryptone, 5% [wt/vol] Bacto Yeast Extract, 5% [wt/vol] NaCl). Appropriate antibiotics were used to select for and maintain plasmids. Antibiotic concentrations used in this study were as follows: for LB+CARB agar, 100 μ g/ml carbenicillin; for LB+CARB liquid medium, 50 μ g/ml carbenicillin, 25 μ g/ml chloramphenicol, and 50 μ g/ml kanamycin. Plasmids were prepared using the Qiagen bacterial miniprep kit (catalog no. 27104; Qiagen).

Plasmid construction. Construction of plasmids used throughout this study was accomplished using a combination of methods, including yeast recombinational cloning (85) and standard restriction enzyme-based cloning. Details of individual plasmid construction are described in Text S1 in the supplemental material.

Generation of optogenetic invertase strain. In order to make an integrable version of the SV40NLS-VP16-CIB1 loxP-KIURA3-loxP SV40NLS-ZIF268DBDCRY2PHR cassette, this cassette was cut from pMM364 using XbaI/PacI and ligated into pMM327. This plasmid was linearized using AatII and transformed into yMM1146 (*Mata trp1 Δ 63 leu2 Δ 1 ura3-52*) to generate yMM1367 (*Mata trp1 Δ 63 leu2 Δ 1 ura3-52 HO::SV40NLS-VP16-CIB1 loxP-KIURA3-loxP SV40NLS-Zif268DBD-CRY2PHR*). The KIURA3 marker was excised from this strain using Cre-mediated recombination as described below to generate yMM1390 (*Mata trp1 Δ 63 leu2 Δ 1 ura3-52 HO::SV40NLS-VP16-CIB1 loxP SV40NLS-Zif268DBD-CRY2PHR*). In order to make the expression of invertase light inducible, the pZF(3BS) promoter replaced the native pSUC2 promoter by amplifying KanMX-rev-pZF(3BS) with oMM768/769 from pMM353, transforming yMM1390 and selecting for G418-resistant colonies. These colonies were further checked by colony PCR and sequencing and for the inability to grow on YP-sucrose in the dark and became strain yMM1406.

Recycling of loxP-flanked markers. The Cre-loxP system was used to recycle the KIURA3 marker flanked by loxP recombination sites (loxP-KIURA3-loxP). Cre-mediated recombination was accomplished by adapting the CRE recombinase-mediated excision protocol from Carter and Delneri (86). The strain yMM1367 (*Mata trp1 Δ 63 leu2 Δ 1 ura3-52 HO::SV40NLS-VP16-CIB1 loxP-KIURA3-loxP SV40NLS-Zif268DBD-CRY2PHR*) was transformed with 0.25 to 0.5 μ g of pMM296 (pSH65, pGAL1-CRE Bleo^r). These transformants were plated onto YPD and then replica plated onto selective medium (YPD plus 10 μ g/ml phleomycin [InvivoGen]) after overnight growth. To express CRE and induce recombination, phleomycin-resistant colonies were selected and grown overnight in 3 ml of YP-raffinose (1% [wt/vol] yeast extract [BD Biosciences],

2% [wt/vol] Bacto peptone [BD Biosciences], and 2% [wt/vol] raffinose [catalog no. 217410; Becton, Dickinson]). The following day, cells were harvested by centrifuging at 3,750 rpm for 5 min, washed in sterile milliQ water, and resuspended in 10 ml of YP-galactose (1% [wt/vol] yeast extract [BD Biosciences], 2% [wt/vol] Bacto-peptone [BD Biosciences], 2% [wt/vol] galactose [catalog no. 216310; BD Biosciences]) at an optical density at 600 nm (OD_{600}) of 0.3. These cultures were incubated at 30°C with shaking for 2 to 3 h. This culture was then diluted and plated on yeast extract-peptone-dextrose (YPD) and then replica plated onto SC-5FOA (25% [wt/vol] g Bacto agar, 6.72% [wt/vol] yeast nitrogen base [YNB], 1% [vol/vol; in milliliters] 20× KS supplement without URA, 2% [vol/vol] glucose, 10 ml of 5-fluoroorotic acid [5FOA] [Zymo Research], 50 mg uracil [catalog no. 103204; MP Biomedicals]). 5FOA-resistant colonies were checked for excision of the KIURA3 marker using colony PCR. Transformants with KIURA3 excised were grown in liquid YPD to saturation twice and then plated on YPD for ~100 colonies per plate. These were replica plated onto YPD plus 10 μ g/ml phleomycin. Phleomycin-sensitive colonies (colonies that had lost the plasmid pMM296) were reconfirmed by colony PCR to have loxed out KIURA3. This generated yMM1390 (*Mata trp1 Δ 63 leu2 Δ 1 ura3-52 HO::SV40NLS-VP16-CIB1 loxP SV40NLS-Zif268DBD-CRY2PHR*).

Blue light induction of yeast cultures in liquid media. For blue light induction experiments in liquid media, light was applied in one of three ways.

(i) Peripheral illumination. Cultures were grown in glass culture tubes on the outside lane of a roller drum at room temperature. Control (dark) samples were put in test tubes wrapped in foil on the inner lane of the roller drum. Three light-emitting diodes (LEDs) outputting 460-nm blue light (catalog no. COM-08718; Sparkfun) were placed at the 3, 9, and 12 o'clock positions of the roller drum and turned on at $T=0$ (~3,000 μ W/cm² at the LED; ~25 μ W/cm² at the sample) as described previously (35, 43).

(ii) Bottom illumination. Cultures growing in glass tubes in a roller drum were directly illuminated from the bottom of the glass culture tube by LEDs mounted into the roller drum. The circuit was composed of three LEDs per tube (catalog no. COM-09662; Sparkfun), resistors of varying strength (catalog no. COM-10969; Sparkfun), and a 12-V power supply (catalog no. 12V-WM-xxA; LEDSupply).

(iii) Light plate apparatus. Cultures were grown in 24-well plates (catalog no. AWLS-303008; ArcticWhite) and placed on a light plate apparatus (LPA) (87). The LPA is a published optogenetic tool that provides programmed illumination to each well of a 24-well plate. We assembled our LPA as described in reference 87 and calibrated as previously described (88, 89).

For all illumination methods, response was assessed by flow (traditional or imaging) cytometry as described below or measurement of optical density. The light output of all light sources was measured and validated with a standard photodiode power sensor (catalog no. S120VC; Thorlabs) and power meter (catalog no. PM100D; Thorlabs) as previously described (43, 88, 89).

Blue light induction of drug resistance or restoration of histidine auxotrophy. To assess blue light induction of drug resistance from a pZF(3B5)-NatMX plasmid, strain yMM1355 (*Mata trp1 Δ 63 leu2 Δ 1 ura3-52 HO::GAL4AD-CIB1 loxP-KLURA3-loxP FLAG(3X)-SV40NLS- Zif268DBD -CRYPHR*) was transformed with the pZF(3B5)-NatMX plasmid (pMM369) or an empty vector control (pMM6). Growth was assessed in the presence of clonNat (nourseothricin, 50 μ g/ml; YPD plates) in either 450-nm blue light (50 μ W/cm²) or the dark by frogging saturated cultures at 1:10 dilution series onto the appropriate plates and growing for 2 days at 30°C in either light or dark. To assess recovery of histidine auxotrophy, strain yMM1295 was transformed with appropriate combinations of pMM284 (ZDBD-CRY2), pMM159 (GAL4AD-CIB1), pMM6 (\emptyset), and pMM7 (\emptyset) and saturated overnight cultures were frogged at 1:10 dilutions onto either SC or SC-Leu-Trp-His. Plates were grown at 30°C under 460-nm blue light or in total darkness. All strains grew on fully supplemented SC in either the light or dark (data not shown). Results for SC-Leu-Trp-His with and without light are shown in Fig. S5A in the supplemental material.

Growth in sucrose media at different blue light intensities. Biological replicates were picked from a single colony on a YPD plate and transferred to a glass culture tube containing 5 ml of YPD medium and grown to saturation overnight in the dark. The saturated culture (1.5 ml) was pelleted by centrifugation (catalog no. EP5401000137; Eppendorf), washed twice with sterile water, and resuspended in sterile MilliQ water to wash out residual media. These concentrated cells were then diluted at 1:100 into 5 ml of SC-sucrose to an OD_{600} of ~0.16 and placed in a roller drum with the corresponding light dose or wrapped in aluminum foil for the no-light control. The cultures were allowed to grow for a total of 48 h with 100 μ l of sample taken every 24 h in order to measure the OD_{600} of the culture using a spectrophotometer (catalog no. 14-385-445; Fisher Scientific).

Time course of growth with light induction in sucrose media. A single yeast colony of strains yMM1406 and yMM1146 was inoculated into 5 ml of YPD and grown overnight to saturation. Of these cultures, 1 ml was pelleted, and the pellet was washed three times with sterile water to wash out residual media. These cultures were then resuspended and diluted in SC-sucrose media to an OD_{600} of 0.05. Each culture was divided into 12 wells of a 24-well plate (2 ml of the diluted cultures) with a glass bead (catalog no. 11-312B; Fisher Scientific) (4 mm) to increase aeration, and the plates were covered with a breathable sealing membrane (catalog no. 9123-6100; USA Scientific) to reduce evaporation. Three light doses were programmed into the LPA with the arbitrary IRIS units of 0, 250, and 500. These correspond to 0 μ W/cm², 2.32 μ W/cm², and 5.01 μ W/cm², respectively. This resulted in a set of four wells for each strain at each light condition. Two of these wells were sampled at each time point, while two were left untouched until the final endpoint measurement to verify that intermediate manipulation of the plate did not inadvertently expose cultures to light. At each time point, 100 μ l of the culture was removed to measure the optical density of the culture, the sealing membrane was replaced, and the plate was returned to the incubator. Optical densities outside of the previously determined linear range of our spectrophotometer were diluted to be in the linear range at a ratio of 1:10 or 1:100 as needed. The experiment run time was 54 h.

Blue light patterning. (i) Patterning of yeast plates with blue light. Yeast strain yMM1406 (optogenetic producer) was inoculated into a 5-ml test tube of YPD and grown overnight to saturation. The next day, the culture was pelleted by microcentrifugation (catalog no. EP5401000137; Eppendorf) at $3,000 \times g$ for 2 min and resuspended in sterile water to wash out residual media from the cell pellet; this process was repeated twice. The final OD_{600} of the yeast cells was measured at 0.119 using a spectrophotometer (catalog no. 14-385-445; Fisher Scientific). Two hundred microliters of the cell suspension was plated on YP-sucrose plates and spread throughout the plate using glass beads (4 mm) (catalog no. 11-312B; Fisher Scientific). The plates were wrapped in sterile, construction paper photomasks with one 6-mm hole placed at the center of the plate and aluminum foil backing to prevent light contamination and control plates of no photomask (full light at $\sim 57 \mu\text{W}/\text{cm}^2$) or complete photomask (no light). The plates were placed under a blue light LED array and allowed to grow at room temperature for a week (until growth appeared to stagnate). Pictures of the plates were taken on day 4 and day 7 with a 28-mm, 12-megapixel camera (iPhone 7).

(ii) Frogger plate patterning. Yeast strain yMM1406 (optogenetic producer) was inoculated into a 5-ml test tube of YPD to grow overnight, the culture was set back to an OD_{600} of 0.219 and grown for a few hours until an OD_{600} of 0.538 was reached. The culture was pelleted in a microcentrifuge (catalog no. EP5401000137; Eppendorf) at $3,000 \times g$ for 2 min and washed three times with sterile water to wash away residual media. The culture was diluted to an OD_{600} of 0.079 measured with a spectrophotometer (catalog no. 14-385-445; Fisher Scientific), and a frogger tool (catalog no. MC48; Dan-Kar Corp.) was used to stamp a large culture plate (catalog no. 431111; Corning) of YP-D agar, a photomask was placed over the bottom of the plate, and only a small section of the plate (2 cm^2) was exposed to light at an intensity $\sim 145 \mu\text{W}/\text{cm}^2$ under a blue light LED array (HQRP New Square 12-inch Grow Light Blue LED 14 W). The light source and plate were placed in 30°C incubator. A lightbox (catalog no. ME456 A4 LED Light Box; Amazon) was used to illuminate the plate from the bottom, and a camera (gel box camera and hood) was used to image the plate on day 4.

(iii) Spot assay with blue light. Yeast strains yMM1146 (wild-type producer), yMM1456 (nonproducer) and yMM1406 (optogenetic producer) were inoculated into a 5-ml test tube of YP-D to grow overnight. Cells were pelleted using a microcentrifuge (Eppendorf, catalog no. EP5401000137) at $3,000 \times g$ for 2 min and washed with YP-sucrose to remove residual media containing dextrose, this was repeated three times. All cultures were diluted to an OD_{600} of 0.04 measured with a spectrophotometer (catalog no. 14-385-445; Fisher Scientific) before plating onto solid YP-sucrose plates (catalog no. BP94501; Fisher Scientific). Onto the lawns of *suc2Δ leu2Δ* cheaters growing on either 0.1 mg/ml or 0.05 mg/ml leucine, we spotted $5 \mu\text{l}$ of either *suc2Δ leu2Δ* cheaters, pZF-SUC2, or wild-type cells. Plates contained leucine concentrations of either 100% (0.1 mg/ml) or 50% (0.05 mg/ml) of the amount used in standard synthetic complete media (59). All plates were spread with $150 \mu\text{l}$ of the yMM1456 (*suc2Δ leu2Δ*) strain with glass beads (4 mm) (catalog no. 11-312B; Fisher Scientific), the beads were removed, and the plate was allowed to dry for 10 min. Then, a $5\text{-}\mu\text{l}$ drop of either yMM1146, -1406, or -1456 was applied to the center of a petri dish and left face-up to dry for another 10 min. The plates were then placed upside down in a 30°C incubator in a single layer under a blue LED light source at an intensity of $145 \mu\text{W}/\text{cm}^2$ (HQRP New Square 12-inch Grow Light Blue LED 14 W) for 7 days. On the seventh day, the pictures were imaged with ChemiDoc imaging system (catalog no. 12003154; Bio-Rad) at an exposure of 0.06 s in the bright-field setting and analyzed using an ImageJ plug-in Clockscan (90).

Quantification of plate growth. (i) Radial intensity traces of patterned plates using Clockscan. The patterned plates were analyzed using a published ImageJ plug-in, Clockscan (90) which outputs averaged radial intensity values for the image.

(ii) Identifying pattern features using custom MATLAB script. We quantify the growth of yeast on a plate from images using a custom MATLAB script that examines intensity versus radius along angular slices through the center of the plate and identifies the bounds of features such as valleys and rings. Because it is hard to accurately identify these features from individual angular slices or the single, composite intensity profile given by a Clockscan (90), we use a bootstrap-based approach to repeatedly identify potential features from randomly selected sets of angular slices and select the most frequently identified potential features as true features.

This starts by roughly identifying the central yeast spot using MATLAB's circle finder and cropping the image around this spot. A polar transformation is then applied to the cropped image to create a polar image where each column of pixels corresponds to an angular slice through the plate. These angular slices are then sampled with replacement to construct a composite image. An intensity profile is generated from each composite image by taking the median intensity value at each radius. The intensity profile is filtered to remove noise, and features are identified from the resulting signal. For example, potential valley bounds are identified as the locations where the derivative of the filtered intensity profile is at its maximum and minimum. This process is repeated for hundreds of composite images to create distributions of potential features. True features are then selected as the mode of these distributions. Using MATLAB's circle find to identify the outer edges of the plate, which we know to be 100 mm across, we then convert the feature measurements to physical units. Code is available upon request.

Flow cytometry. Gene expression in response to blue light was assayed using fluorescent reporters and either traditional or imaging flow cytometry. Traditional flow cytometry was performed on a BD Biosciences LSR II flow cytometer (488-nm laser and 505LP dichroic filter). The flow cytometry data were then analyzed using custom Matlab scripts. Imaging cytometry was done with the ImageStream MarkII, and analysis was completed using the IDEAS software or custom Matlab/ImageJ scripts modified from those described in reference 29.

All samples from culture tubes were prepared by diluting yeast cell culture (250 to $500 \mu\text{l}$) into $800 \mu\text{l}$ of ice-cold phosphate-buffered saline (PBS) plus 0.1% Tween 20. Samples were kept on ice or at

4°C until being analyzed. Samples from the light plate apparatus were taken by transferring 50 μ l of culture from each well of the LPA to a well in a 96-well plate containing 150 μ l of PBS plus 0.1% Tween 20. Samples run on the LPA were measured without sonication. Samples grown in glass culture tubes were sonicated with 10 bursts of 0.5 s each once diluted in PBS and prior to flow cytometry.

SUPPLEMENTAL MATERIAL

Supplemental material is available online only.

TEXT S1, DOCX file, 0.04 MB.

FIG S1, EPS file, 1.9 MB.

FIG S2, TIF file, 0.7 MB.

FIG S3, EPS file, 2 MB.

FIG S4, EPS file, 1.5 MB.

FIG S5, TIF file, 1.5 MB.

FIG S6, EPS file, 1.4 MB.

FIG S7, TIF file, 1.7 MB.

FIG S8, TIF file, 0.8 MB.

TABLE S1, DOCX file, 0.1 MB.

ACKNOWLEDGMENTS

This work was financially supported by the National Institutes of Health (R35GM128873), the National Science Foundation (2045493), and a Lewis-Sigler Fellowship from Princeton University (M.N.M.). Flow cytometry was enabled by the University of Wisconsin Carbone Cancer Center Support Grant P30 CA014520 as well as the Princeton Flow Cytometry Resource Facility. Megan Nicole McClean holds a Career Award at the Scientific Interface from the Burroughs Wellcome Fund. Neydis Moreno Morales was supported by a short-term Genomic Sciences Training Program NHGRI Training Grant (5T32HG002760) and the Science and Medicine Graduate Research Scholars (SciMed GRS) program at the University of Wisconsin—Madison.

N.M.M., C.J.S., and M.T.P. designed experiments and performed experiments. N.M.M., C.J.S., and M.T.P. performed molecular cloning and strain construction. K.S. wrote image analysis software. N.M.M. and M.N.M. analyzed data and wrote the paper. N.M.M., C.J.S., M.T.P., K.S., and M.N.M. edited and approved the manuscript. M.N.M. supervised the project.

REFERENCES

1. Stubbendieck RM, Vargas-Bautista C, Straight PD. 2016. Bacterial communities: interactions to scale. *Front Microbiol* 7:1234. <https://doi.org/10.3389/fmicb.2016.01234>.
2. Ponomarova O, Patil KR. 2015. Metabolic interactions in microbial communities: untangling the Gordian knot. *Curr Opin Microbiol* 27:37–44. <https://doi.org/10.1016/j.mib.2015.06.014>.
3. Nadell CD, Drescher K, Foster KR. 2016. Spatial structure, cooperation and competition in biofilms. *Nat Rev Microbiol* 14:589–600. <https://doi.org/10.1038/nrmicro.2016.84>.
4. Gralka M, Szabo R, Stocker R, Cordero OX. 2020. Trophic interactions and the drivers of microbial community assembly. *Curr Biol* 30:R1176–R1188. <https://doi.org/10.1016/j.cub.2020.08.007>.
5. Friedman J, Gore J. 2017. Ecological systems biology: the dynamics of interacting populations. *Curr Opin Syst Biol* 1:114–121. <https://doi.org/10.1016/j.coisb.2016.12.001>.
6. Germerodt S, Bohl K, Lück A, Pande S, Schröter A, Kaleta C, Schuster S, Kost C. 2016. Pervasive selection for cooperative cross-feeding in bacterial communities. *PLoS Comput Biol* 12:e1004986. <https://doi.org/10.1371/journal.pcbi.1004986>.
7. Mitri S, Foster KR. 2013. The genotypic view of social interactions in microbial communities. *Annu Rev Genet* 47:247–273. <https://doi.org/10.1146/annurev-genet-111212-133307>.
8. Smith P, Schuster M. 2019. Public goods and cheating in microbes. *Curr Biol* 29:R442–R447. <https://doi.org/10.1016/j.cub.2019.03.001>.
9. Barnett JA. 2000. A history of research on yeasts 2: Louis Pasteur and his contemporaries, 1850–1880. *Yeast (Chichester, Engl)* 16:755–771. [https://doi.org/10.1002/1097-0061\(20000615\)16:8<755::AID-YEA587>3.0.CO;2-4](https://doi.org/10.1002/1097-0061(20000615)16:8<755::AID-YEA587>3.0.CO;2-4).
10. Brown AJ. 1902. Enzyme action. *J Chem Soc Trans* 81:373–388. <https://doi.org/10.1039/CT9028100373>.
11. Michaelis L, Menten M. 1913. Kinetik de Invertinwirkung. *Biochem Z* 49: 333–369.
12. Carlson M, Botstein D. 1983. Organization of the SUC gene family in *Saccharomyces*. *Mol Cell Biol* 3:351–359. <https://doi.org/10.1128/mcb.3.3.351-359.1983>.
13. Naumov GI, Naumova ES. 2010. Comparative genetics of yeasts: a novel beta-fructosidase gene SUC8 in *Saccharomyces cerevisiae*. *Genetika* 46: 364–372. (In Russian.)
14. Carlson M, Celenza JL, Eng FJ. 1985. Evolution of the dispersed SUC gene family of *Saccharomyces* by rearrangements of chromosome telomeres. *Mol Cell Biol* 5:2894–2902. <https://doi.org/10.1128/MCB.5.11.2894>.
15. Carlson M, Osmond BC, Botstein D. 1981. Mutants of yeast defective in sucrose utilization. *Genetics* 98:25–40. <https://doi.org/10.1093/genetics/98.1.25>.
16. Carlson M, Botstein D. 1982. Two differentially regulated mRNAs with different 5' ends encode secreted with intracellular forms of yeast invertase. *Cell* 28:145–154. [https://doi.org/10.1016/0092-8674\(82\)90384-1](https://doi.org/10.1016/0092-8674(82)90384-1).
17. Gore J, Youk H, Van Oudenaarden A. 2009. Snowdrift game dynamics and facultative cheating in yeast. *Nature* 459:253–256. <https://doi.org/10.1038/nature07921>.
18. Esmon PC, Esmon BE, Schauer IE, Taylor A, Schekman R. 1987. Structure, assembly, and secretion of octameric invertase. *J Biol Chem* 262: 4387–4394. [https://doi.org/10.1016/S0021-9258\(18\)61360-2](https://doi.org/10.1016/S0021-9258(18)61360-2).
19. Tammi M, Ballou L, Taylor A, Ballou CE. 1987. Effect of glycosylation on yeast invertase oligomer stability. *J Biol Chem* 262:4395–4401. [https://doi.org/10.1016/S0021-9258\(18\)61361-4](https://doi.org/10.1016/S0021-9258(18)61361-4).

20. Greig D, Travisano M. 2004. The Prisoner's Dilemma and polymorphism in yeast SUC genes. *Proc Biol Sci* 271(Suppl 3):S25–S26. <https://doi.org/10.1098/rsbl.2003.0083>.
21. Misevic D, Frénoy A, Parsons DP, Taddei F. 2012. Effects of public good properties on the evolution of cooperation. *Artif Life Conf Proc* 24:218–225.
22. Allison S. 2005. Cheaters, diffusion and nutrients constrain decomposition by microbial enzymes in spatially structured environments. *Ecol Lett* 8: 626–635. <https://doi.org/10.1111/j.1461-0248.2005.00756.x>.
23. Kümmerli R, Schiessl KT, Waldvogel T, McNeill K, Ackermann M. 2014. Habitat structure and the evolution of diffusible siderophores in bacteria. *Ecol Lett* 17:1536–1544. <https://doi.org/10.1111/ele.12371>.
24. Kummerli R, Griffin A, West S, Buckling A, Harrison F. 2009. Viscous medium promotes cooperation in the pathogenic bacterium *Pseudomonas aeruginosa*. *Proc Biol Sci* 276:3531–3538. <https://doi.org/10.1098/rspb.2009.0861>.
25. Julou T, Mora T, Guillon L, Croquette V, Schalk IJ, Bensimon D, Desprat N. 2013. Cell–cell contacts confine public goods diffusion inside *Pseudomonas aeruginosa* clonal microcolonies. *Proc Natl Acad Sci U S A* 110: 12577–12582. <https://doi.org/10.1073/pnas.1301428110>.
26. Momeni B, Waite AJ, Shou W. 2013. Spatial self-organization favors heterotypic cooperation over cheating. *Elife* 2:e00960. <https://doi.org/10.7554/eLife.00960>.
27. Lindsay RJ, Pawlowska BJ, Gudelj I. 2018. When increasing population density can promote the evolution of metabolic cooperation. *ISME J* 12: 849–859. <https://doi.org/10.1038/s41396-017-0016-6>.
28. Nadell CD, Foster KR, Xavier JB. 2010. Emergence of spatial structure in cell groups and the evolution of cooperation. *PLoS Comput Biol* 6: e1000716. <https://doi.org/10.1371/journal.pcbi.1000716>.
29. Su Q, Li A, Wang L. 2017. Spatial structure favors cooperative behavior in the snowdrift game with multiple interactive dynamics. *Phys Stat Mech Its Appl* 468:299–306. <https://doi.org/10.1016/j.physa.2016.10.095>.
30. Kim HJ, Boedicker JQ, Choi JW, Ismagilov RF. 2008. Defined spatial structure stabilizes a synthetic multispecies bacterial community. *Proc Natl Acad Sci U S A* 105:18188–18193. <https://doi.org/10.1073/pnas.0807935105>.
31. Koschwanez JH, Foster KR, Murray AW. 2013. Improved use of a public good selects for the evolution of undifferentiated multicellularity. *Elife* 2: e00367. <https://doi.org/10.7554/eLife.00367>.
32. Cavaliere M, Feng S, Soyer OS, Jiménez JI. 2017. Cooperation in microbial communities and their biotechnological applications. *Environ Microbiol* 19:2949–2963. <https://doi.org/10.1111/1462-2920.13767>.
33. Rodríguez Amor D, Dal Bello M. 2019. Bottom-up approaches to synthetic cooperation in microbial communities. *Life* 9:22. <https://doi.org/10.3390/life9010022>.
34. Salinas F, Rojas V, Delgado V, Agosin E, Larrondo LF. 2017. Optogenetic switches for light-controlled gene expression in yeast. *Appl Microbiol Biotechnol* 101:2629–2640. <https://doi.org/10.1007/s00253-017-8178-8>.
35. Melendez J, Patel M, Oakes BL, Xu P, Morton P, McClean MN. 2014. Real-time optogenetic control of intracellular protein concentration in microbial cell cultures. *Integr Biol (Camb)* 6:366–372. <https://doi.org/10.1039/c3ib40102b>.
36. Carrasco-López C, García-Echauri SA, Kichuk T, Avalos JL. 2020. Optogenetics and biosensors set the stage for metabolic cybergenetics. *Curr Opin Biotechnol* 65:296–309. <https://doi.org/10.1016/j.copbio.2020.07.012>.
37. Milias-Argentis A, Summers S, Stewart-Ornstein J, Zuleta I, Pincus D, El-Samad H, Khammash M, Lygeros J. 2011. In silico feedback for in vivo regulation of a gene expression circuit. *Nat Biotechnol* 29:1114–1116. <https://doi.org/10.1038/nbt.2018>.
38. Figueroa D, Rojas V, Romero A, Larrondo LF, Salinas F. 2021. The rise and shine of yeast optogenetics. *Yeast* 38:131–146. <https://doi.org/10.1002/yea.3529>.
39. Burmeister A, Akhtar Q, Hollmann L, Tenhaef N, Hilgers F, Hogenkamp F, Sokolowsky S, Marienhagen J, Noack S, Kohlheyer D, Grünberger A. 2021. (Optochemical) control of synthetic microbial coculture interactions on a microcolony level. *ACS Synth Biol* 10:1308–1319. <https://doi.org/10.1021/acssynbio.0c00382>.
40. Huang Y, Xia A, Yang G, Jin F. 2018. Bioprinting living biofilms through optogenetic manipulation. *ACS Synth Biol* 7:1195–1200. <https://doi.org/10.1021/acssynbio.8b00003>.
41. Pirhanov A, Bridges CM, Goodwin RA, Guo Y-S, Furrer J, Shor LM, Gage DJ, Cho YK. 2021. Optogenetics in *Sinorhizobium meliloti* enables spatial control of exopolysaccharide production and biofilm structure. *ACS Synth Biol* 10:345–356. <https://doi.org/10.1021/acssynbio.0c00498>.
42. McIsaac RS, Oakes BL, Wang X, Dummit KA, Botstein D, Noyes MB. 2013. Synthetic gene expression perturbation systems with rapid, tunable, single-gene specificity in yeast. *Nucleic Acids Res* 41:e57. <https://doi.org/10.1093/nar/gks1313>.
43. An-Adirekku JM, Stewart CJ, Geller SH, Patel MT, Melendez J, Oakes BL, Noyes MB, McClean MN. 2020. A yeast optogenetic toolkit (yOTK) for gene expression control in *Saccharomyces cerevisiae*. *Biotechnol Bioeng* 117:886–893. <https://doi.org/10.1002/bit.27234>.
44. Lee ME, DeLoache WC, Cervantes B, Dueber JE. 2015. A highly characterized yeast toolkit for modular, multipart assembly. *ACS Synth Biol* 4: 975–986. <https://doi.org/10.1021/sb500366v>.
45. Gueldener U, Heinisch J, Koehler GJ, Voss D, Hegemann JH. 2002. A second set of loxP marker cassettes for Cre-mediated multiple gene knock-outs in budding yeast. *Nucleic Acids Res* 30:e23. <https://doi.org/10.1093/nar/30.6.e23>.
46. Voth WP, Richards JD, Shaw JM, Stillman DJ. 2001. Yeast vectors for integration at the HO locus. *Nucleic Acids Res* 29:E59. <https://doi.org/10.1093/nar/29.12.e59>.
47. Baganz F, Hayes A, Marren D, Gardner DC, Oliver SG. 1997. Suitability of replacement markers for functional analysis studies in *Saccharomyces cerevisiae*. *Yeast* (Chichester, Engl) 13:1563–1573. [https://doi.org/10.1002/\(SICI\)1097-0061\(199712\)13:16<1563::AID-YEA240>3.0.CO;2-6](https://doi.org/10.1002/(SICI)1097-0061(199712)13:16<1563::AID-YEA240>3.0.CO;2-6).
48. Redden H, Morse N, Alper HS. 2015. The synthetic biology toolbox for tuning gene expression in yeast. *FEMS Yeast Res* 15:1–10. <https://doi.org/10.1111/1567-1364.12188>.
49. Greger IH, Proudfoot NJ. 1998. Poly(A) signals control both transcriptional termination and initiation between the tandem GAL10 and GAL7 genes of *Saccharomyces cerevisiae*. *EMBO J* 17:4771–4779. <https://doi.org/10.1093/emboj/17.16.4771>.
50. Wach A, Brachat A, Pöhlmann R, Philippsen P. 1994. New heterologous modules for classical or PCR-based gene disruptions in *Saccharomyces cerevisiae*. *Yeast* 10:1793–1808. <https://doi.org/10.1002/yea.320101310>.
51. Allee WC, Emerson A, Park O, Park T, Schmidt KP. 1967. Principles of animal ecology. W. B. Saunders Company, Philadelphia, PA.
52. Dai L, Vorselen D, Korolev KS, Gore J. 2012. Generic indicators for loss of resilience before a tipping point leading to population collapse. *Science* 336:1175–1177. <https://doi.org/10.1126/science.1219805>.
53. Sanchez A, Gore J. 2013. Feedback between population and evolutionary dynamics determines the fate of social microbial populations. *PLoS Biol* 11:e1001547. <https://doi.org/10.1371/journal.pbio.1001547>.
54. Lauterjung KR, Morales NM, McClean MN. 2020. Secrete to beat the heat. *Nat Microbiol* 5:883–884. <https://doi.org/10.1038/s41564-020-0748-3>.
55. Basu S, Gerchman Y, Collins CH, Arnold FH, Weiss R. 2005. A synthetic multicellular system for programmed pattern formation. *Nature* 434: 1130–1134. <https://doi.org/10.1038/nature03461>.
56. Murray JD. 2003. *Mathematical biology II: spatial models and biomedical applications*, vol 18. Springer-Verlag, New York, NY.
57. Kong W, Blanchard AE, Liao C, Lu T. 2017. Engineering robust and tunable spatial structures with synthetic gene circuits. *Nucleic Acids Res* 45: 1005–1014. <https://doi.org/10.1093/nar/gkw1045>.
58. Tabor JJ, Salis HM, Simpson ZB, Chevalier AA, Levskaya A, Marcotte EM, Voigt CA, Ellington AD. 2009. A synthetic genetic edge detection program. *Cell* 137:1272–1281. <https://doi.org/10.1016/j.cell.2009.04.048>.
59. Cold Spring Harbor Protocols. 2016. Synthetic complete (SC) medium. *Cold Spring Harb Protoc* <https://doi.org/10.1101/pdb.rec090589>.
60. Sarokin L, Carlson M. 1985. Upstream region of the SUC2 gene confers regulated expression to a heterologous gene in *Saccharomyces cerevisiae*. *Mol Cell Biol* 5:2521–2526. <https://doi.org/10.1128/MCB.5.10.2521>.
61. Neigeborn L, Carlson M. 1984. Genes affecting the regulation of SUC2 gene expression by glucose repression in *Saccharomyces cerevisiae*. *Genetics* 108:845–858. <https://doi.org/10.1093/genetics/108.4.845>.
62. Cordero OX, Datta MS. 2016. Microbial interactions and community assembly at microscales. *Curr Opin Microbiol* 31:227–234. <https://doi.org/10.1016/j.mib.2016.03.015>.
63. Dal Co A, van Vliet S, Kiviet DJ, Schlegel S, Ackermann M. 2020. Short-range interactions govern the dynamics and functions of microbial communities. *Nat Ecol Evol* 4:366–375. <https://doi.org/10.1038/s41559-019-1080-2>.
64. Donaldson GP, Lee SM, Mazmanian SK. 2016. Gut biogeography of the bacterial microbiota. *Nat Rev Microbiol* 14:20–32. <https://doi.org/10.1038/nrmicro3552>.
65. Gupta S, Ross TD, Gomez MM, Grant JL, Romero PA, Venturelli OS. 2020. Investigating the dynamics of microbial consortia in spatially structured environments. *Nat Commun* 11:2418. <https://doi.org/10.1038/s41467-020-16200-0>.
66. Alnahhas RN, Winkle JJ, Hirning AJ, Karamched B, Ott W, Josić K, Bennett MR. 2019. Spatiotemporal dynamics of synthetic microbial consortia in

- microfluidic devices. *ACS Synth Biol* 8:2051–2058. <https://doi.org/10.1021/acssynbio.9b00146>.
67. Burmeister A, Grünberger A. 2020. Microfluidic cultivation and analysis tools for interaction studies of microbial co-cultures. *Curr Opin Biotechnol* 62:106–115. <https://doi.org/10.1016/j.copbio.2019.09.001>.
 68. Burmeister A, Hilgers F, Langner A, Westerwalbesloh C, Kerkhoff Y, Tenhaef N, Drepper T, Kohlheyer D, von Lieres E, Noack S, Grünberger A. 2018. A microfluidic co-cultivation platform to investigate microbial interactions at defined microenvironments. *Lab Chip* 19:98–110. <https://doi.org/10.1039/c8lc00977e>.
 69. Saha A, Johnston TG, Shafraneck RT, Goodman CJ, Zalatan JG, Storti DW, Ganter MA, Nelson A. 2018. Additive manufacturing of catalytically active living materials. *ACS Appl Mater Interfaces* 10:13373–13380. <https://doi.org/10.1021/acscami.8b02719>.
 70. Hynes WF, Chacón J, Segrè D, Marx CJ, Cady NC, Harcombe WR. 2018. Bio-printing microbial communities to examine interspecies interactions in time and space. *Biomed Phys Eng Express* 4:e055010. <https://doi.org/10.1088/2057-1976/aad544>.
 71. Merrin J, Leibler S, Chuang JS. 2007. Printing multistrain bacterial patterns with a piezoelectric inkjet printer. *PLoS One* 2:e663. <https://doi.org/10.1371/journal.pone.0000663>.
 72. Hartsough LA, Park M, Kotlajich MV, Lazar JT, Han B, Lin C-CJ, Musteata E, Gambill L, Wang MC, Tabor JJ. 2020. Optogenetic control of gut bacterial metabolism to promote longevity. *Elife* 9:e56849. <https://doi.org/10.7554/eLife.56849>.
 73. Pouzet S, Banderas A, Le Bec M, Lautier T, Truan G, Hersen P. 2020. The promise of optogenetics for bioproduction: dynamic control strategies and scale-up instruments. *Bioengineering* 7:151. <https://doi.org/10.3390/bioengineering7040151>.
 74. Zhao EM, Zhang Y, Mehl J, Park H, Lalwani MA, Toettcher JE, Avalos JL. 2018. Optogenetic regulation of engineered cellular metabolism for microbial chemical production. *Nature* 555:683–687. <https://doi.org/10.1038/nature26141>.
 75. Ohlendorf R, Vidavski RR, Eldar A, Moffat K, Möglich A. 2012. From dusk till dawn: one-plasmid systems for light-regulated gene expression. *J Mol Biol* 416:534–542. <https://doi.org/10.1016/j.jmb.2012.01.001>.
 76. Levskaya A, Chevalier AA, Tabor JJ, Simpson ZB, Lavery LA, Levy M, Davidson EA, Scouras A, Ellington AD, Marcotte EM, Voigt CA. 2005. Synthetic biology: engineering *Escherichia coli* to see light. *Nature* 438:441–442. <https://doi.org/10.1038/nature04405>.
 77. Brenner K, You L, Arnold FH. 2008. Engineering microbial consortia: a new frontier in synthetic biology. *Trends Biotechnol* 26:483–489. <https://doi.org/10.1016/j.tibtech.2008.05.004>.
 78. Chen Y, Kim JK, Hirning AJ, Josić K, Bennett MR. 2015. Emergent genetic oscillations in a synthetic microbial consortium. *Science* 349:986–989. <https://doi.org/10.1126/science.aaa3794>.
 79. Marchand N, Collins CH. 2013. Peptide-based communication system enables *Escherichia coli* to *Bacillus megaterium* interspecies signaling. *Biotechnol Bioeng* 110:3003–3012. <https://doi.org/10.1002/bit.24975>.
 80. Kouya T, Ishiyama Y, Tanaka T, Taniguchi M. 2013. Evaluation of positive interaction for cell growth between *Bifidobacterium adolescentis* and *Propionibacterium freudenreichii* using a co-cultivation system with two microfiltration modules. *J Biosci Bioeng* 115:189–192. <https://doi.org/10.1016/j.jbiosc.2012.09.005>.
 81. Lovelett RJ, Zhao EM, Lalwani MA, Toettcher JE, Kevrekidis IG, Avalos JL. 2021. Dynamical modeling of optogenetic circuits in yeast for metabolic engineering applications. *ACS Synth Biol* 10:219–227. <https://doi.org/10.1021/acssynbio.0c00372>.
 82. Gietz RD, Schiestl RH. 2007. High-efficiency yeast transformation using the LiAc/SS carrier DNA/PEG method. *Nat Protoc* 2:31–34. <https://doi.org/10.1038/nprot.2007.13>.
 83. Harju S, Fedosyuk H, Peterson KR. 2004. Rapid isolation of yeast genomic DNA: Bust n' Grab. *BMC Biotechnol* 4:8. <https://doi.org/10.1186/1472-6750-4-8>.
 84. Sambrook J, Russell DW. 2006. The Inoue method for preparation and transformation of competent *E. coli*: “ultra-competent” cells. *Cold Spring Harb Protoc* <https://doi.org/10.1101/pdb.prot3944>.
 85. Andersen EC. 2011. PCR-directed in vivo plasmid construction using homologous recombination in baker's yeast. *Methods Mol Biol (Clifton NJ)* 772:409–421. https://doi.org/10.1007/978-1-61779-228-1_24.
 86. Carter Z, Delneri D. 2010. New generation of loxP-mutated deletion cassettes for the genetic manipulation of yeast natural isolates. *Yeast* 27:765–775. <https://doi.org/10.1002/yea.1774>.
 87. Gerhardt KP, Olson EJ, Castillo-Hair SM, Hartsough LA, Landry BP, Ekness F, Yokoo R, Gomez EJ, Ramakrishnan P, Suh J, Savage DF, Tabor JJ. 2016. An open-hardware platform for optogenetics and photobiology. *Sci Rep* 6:35363. <https://doi.org/10.1038/srep35363>.
 88. Grødem EO, Sweeney K, McClean MN. 2020. Automated calibration of opto-plate LEDs to reduce light dose variation in optogenetic experiments. *Bio-techniques* 69:313–316. <https://doi.org/10.2144/btn-2020-0077>.
 89. Sweeney K, Moreno Morales N, Burmeister Z, Nimunkar AJ, McClean MN. 2019. Easy calibration of the Light Plate Apparatus for optogenetic experiments. *MethodsX* 6:1480–1488. <https://doi.org/10.1016/j.mex.2019.06.008>.
 90. Dobretsov M, Petkau G, Hayar A, Petkau E. 2017. Clock scan protocol for Image analysis: ImageJ plugins. *J Vis Exp* 2017:55819. <https://doi.org/10.3791/55819>.